International Journal of Recent Technology and Engineering (IJRTE)
ISSN: 2277-3878, Volume-8 Issue-4, November 2019

Effect of the Parametric Variations of Semiconductor Screen on Line Parameters and Wave Properties of Underground Cable

Swarnankur Ghosh, Supriyo Das

Abstract*: Detection and understanding of different high frequency phenomenon in multilayered underground (UG) cable require a thorough study of wave propagation mechanism which is governed by the line parameters of the cable. Line parameters are the functions of cable geometric and electromagnetic properties. Therefore the inclusion of semiconducting screen in cable structure influences the line parameters as well as wave properties of the cable. This paper aims to investigate the effects of the variation of different geometric and electrical properties of the semiconducting screen on line parameters as well as wave propagation characteristics of UG cable over a wide range of frequency. The complete impedance matrix of cable considering the effect of the semiconducting screen is derived using loop current analysis without invoking the theory of a double-layered conductor system. A comparative analysis on the effect of parametric variations of the semiconducting screen on line parameters as well as wave properties between the cable with and without semiconducting screen over a wide range of frequency is performed. This analysis indicates that the wave properties like attenuation or phase velocity are considerably influenced by inclusions of the semiconducting screen in cable structure, especially at high frequency.

***Keywords* : Loop Current, Mesh and phase domain, Skin Depth, Attenuation Constant.**

I. INTRODUCTION

Like transmission line, underground (UG) power cable is also susceptible to different high frequency phenomenon which propagates as a wave through it. As the wave propagation mechanism in a cable is governed by its primary line parameters, cable geometry and material properties have a direct influence on its wave properties. Therefore the inclusion of semiconducting screen in cable structure has a considerable effect on primary line parameters which in turn influences the wave properties of the cable. Determination of wave properties of UG cable based on cable primary line parameters requires the derivation of a complete model of impedance and admittance of the multilayered cable which was first successfully done in [1] based on the electromagnetic analysis of coaxial cylinder [2]. Though this model has widespread applications in the study of high frequency behavior of multilayered cable [3-6], it is only suitable for cable structure containing alternate conducting and insulating layers [3]. However, most of the practical cable uses a semiconducting screen between conducting and insulating layers which has considerable effects on cable line parameters as well as wave properties [7, 8]. Therefore the need for modification in the existing impedance and admittance model [1] of UG cable to include the effect of the semiconducting screen was arisen. After several attempts [9-12], a complete and explicit mathematical model of cable impedance considering the effect of the semiconducting layer was first derived in [13] by solving Maxwell's equations for a two-layered conductor which was later verified using circuit and numerical approach [14, 15]. These works and subsequent works [10, 16-20] investigated the effects of the variation of semiconductor resistivity and dielectric properties on line parameters as well as wave properties of the cable considering different factors like frequency, pressure and temperatures of semiconductor sample, etc. both theoretically and experimentally. These investigations were mainly emphasized on reporting the role of the materialistic properties of the semiconducting screen on attenuation characteristic and deformation of propagated signal, especially at high frequency.

This paper aims to understand and analyze the effects of the variation of electrical and geometric properties of the semiconducting screen on all three primary line parameters namely resistive, inductive and capacitive part of the UG cable over a wide range of frequency. The influence of different parametric variations of the semiconducting screen on wave properties of the cable is also studied. The line parameters, as well as wave properties of the cable with semiconducting screen, are obtained from the expressions of impedance and admittance of the cable. The expressions of impedance and admittance are derived using the loop current method of circuit analysis. This method provides a way to incorporate the effect of the semiconducting screen in the expressions of cable impedance directly without recalling the theory of double-layered conductor theory as done in [13, 14].

Manuscript published on November 30, 2019.
* Correspondence Author
Swarnankur Ghosh*, Department of Electrical Engineering, National Institute of Technology Meghalaya, Laitumkhrah, Shillong, India. Email: swarnankur.ghosh@nitm.ac.in
Supriyo Das, Department of Electrical Engineering, National Institute of Technology Meghalaya, Laitumkhrah, Shillong, India. Email: supriyo@nitm.ac.in

A comparative analysis between the cable with and without semiconducting screen based on the effect of parametric variations of the semiconducting screen on line parameters and wave properties of the cable is performed. The analysis shows that by varying electrical and geometric properties of the semiconducting screen in cable considerable changes in the line parameters can be made especially at high frequency compared to that of cable without semiconducting screen which in turn influences the wave properties. Also, by

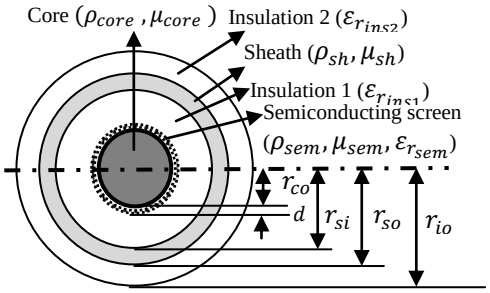

Fig. 1.Cross-section of UG cable with semiconductor screen

varying different parameters of the semiconducting screen wave properties of the cable can be improved.

II. CABLE LINE PARAMETERS

A. Impedance of cable without semiconducting screen

Considering a single core (SC) coaxial cable without semiconducting screen whose impedance matrix ($[Z]_{mesh}$) in mesh domain is given by [1],

$$[Z]_{mesh} = \begin{bmatrix} Z_{l_{11}} & Z_{l_{12}} \\ Z_{l_{21}} & Z_{l_{22}} \end{bmatrix} \quad (1)$$

where,

$Z_{l_{11}}$ = Self impedance of internal loop between core and sheath = $\mathfrak{z}_{core_{out}} + \mathfrak{z}_{sh_{in}} + \mathfrak{z}_{ins_1}$ (1.a)

$Z_{l_{12}}$ = Mutual impedance of loop between core & sheath due to core current

= $Z_{l_{21}}$ = Mutual impedance of loop between core & sheath due to sheath current = $-\mathfrak{z}_{sh_m}$ (1.b)

$Z_{l_{22}}$ == Self impedance of internal loop between the sheath and earth = $\mathfrak{z}_{sh_{out}} + Z_e + \mathfrak{z}_{ins_2}$ (1.c)

where, $\mathfrak{z}_{core_{out}}$ is the per unit length outer surface impedance of the core, $\mathfrak{z}_{sh_{out}}$ & $\mathfrak{z}_{sh_{in}}$ are per unit length impedance of sheath outer and inner surface respectively and $\mathfrak{z}_{sh_m}$ per unit length mutual impedance between the surfaces of the sheath. The surface and mutual impedances of each conducting layer of coaxial cable structure is given by [2],

Z_{in}= Inner surface impedance of the cylindrical conductor

$$= \frac{m\rho_c}{2\pi r_{in} D}\{I_0(mr_{in})K_1(mr_{out}) + K_0(mr_{in})I_1(mr_{out})\} \quad (2)$$

Z_{out} = Outer surface impedance of the cylindrical conductor

$$= \frac{m\rho_c}{2\pi r_{out} D}\{I_0(mr_{out})K_1(mr_{in}) + K_0(mr_{out})I_1(mr_{in})\} \quad (3)$$

Z_m=Mutual impedance between inner & outer surfaces

$$= \frac{\rho_c}{2\pi r_{out} r_{in} D} \quad (4)$$

where,

D= $\{I_1(mr_{out})\, K_1(mr_{in}) - K_1(mr_{out})I_1(mr_{in})\}$

$m = \sqrt{\frac{j\omega\mu_c}{\rho_c}}$ = Reciprocal of skin depth

ρ_c& μ_c are the resistivity and permeability respectively, and r_{in} & r_{out} are respectively the inner and outer radius of the cylindrical conductor.

I_0, I_1, K_0 and K_1 are the modified Bessel's Functions.

The impedance of insulation between conducting layers, i.e., $\mathfrak{z}_{ins}$ & $z_{\ldots}$ are given by

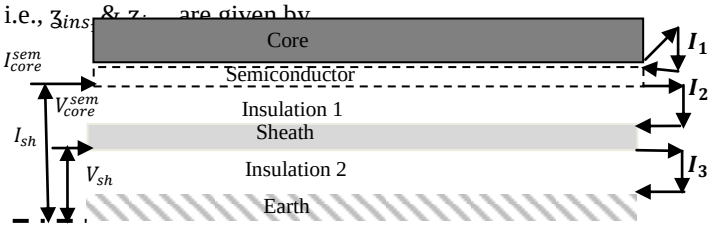

Fig. 2. Loop & phase quantities in UG cable with semiconductor

$$= j\omega\frac{\mu_0}{2\pi}\ln\frac{r_{ins_{out}}}{r_{ins_{in}}} \quad (5)$$

where $r_{ins_{in}}$ & $r_{ins_{out}}$ are the inner and outer radius respectively of the insulating layer.

Z_e=Earth impedance [1]

B. Impedance of cable with semiconducting screen

Considering the semiconducting screen is present in cable structure as shown in Fig.1, the cable impedance matrix, given by (1), needs to be modified to include the effect of the semiconducting screen. It is evident from Fig.1 that semiconducting screen on core outer surface with no insulation between them forms a double-layered conductor system.

In this work, an approach based on loop current analysis is adopted, which can directly include the correction terms for incorporating the effect of the semiconducting screen in the expressions of cable impedances in mesh domain. This method provides a circuit-based approach to calculate the effective impedance of conductor-semiconductor assembly present in the cable without invoking the electromagnetic theory of determining component impedances of the double-layered conductor as done in [13,14].

Fig. 2 shows the longitudinal cross-section of the cable with the semiconducting screen. Three local loops are assumed to be formed between the core & semiconducting screen, semiconducting screen & sheath and sheath & Earth as shown in Fig.2. The respective loop currents and loop voltages are assumed to be I_1, I_2 & I_3 and ΔV_1, ΔV_2 & ΔV_3. The per unit length impedance of outer and inner surface, as well as mutual impedance between the surfaces of the semiconducting screen, are denoted as $\mathfrak{z}_{sem_{in}}$, $\mathfrak{z}_{sem_{out}}$ & $\mathfrak{z}_{sem_m}$ respectively which can also be determined using (2) to (4). Then the loop equations, neglecting earth impedance as per [13], are given by,

ΔV_1=$I_1(\mathfrak{z}_{core_{out}} + \mathfrak{z}_{sem_{in}}) - I_2\mathfrak{z}_{sem_m}$ (6)

ΔV_2=$I_2(\mathfrak{z}_{sem_{out}} + \mathfrak{z}_{sh_{in}} + \mathfrak{z}_{ins1}) - I_1\mathfrak{z}_{sem_m} - I_3\mathfrak{z}_{sh_m}$ (7)

Retrieval Number: D7452118419/2019©BEIESP
DOI:10.35940/ijrte.D7452.118419
Journal Website: www.ijrte.org

Published By:
Blue Eyes Intelligence Engineering and Sciences Publication (BEIESP)

$$\Delta V_3 = I_3\left(\mathfrak{Z}_{sh_{out}} + \mathfrak{Z}_{ins2} + Z_e\right) - I_2\mathfrak{Z}_{sh_m} \quad (8)$$

But with no insulation between the core and semiconducting screen, they are at the same potential, thus $\Delta V_1 = 0$. Hence from (6), we get,

$$I_1 = I_2 \frac{\mathfrak{Z}_{sem_m}}{\left(\mathfrak{Z}_{core_{out}} + \mathfrak{Z}_{sem_{in}}\right)} \quad (9)$$

Substituting the value of I_1 in (7) gives-

$$\Delta V_2 = I_2\left(\mathfrak{Z}_{sem_{out}} - \frac{\mathfrak{Z}_{sem_m}^{\ 2}}{\mathfrak{Z}_{core_{out}} + \mathfrak{Z}_{sem_{in}}} + \mathfrak{Z}_{sh_{in}} + \mathfrak{Z}_{ins1}\right) - I_3\mathfrak{Z}_{sh_m} \quad (10)$$

Therefore, from (10), the self impedance of loop 1 ($Z_{l_{11}}^{sem}$) etween core-semiconductor assembly and sheath is,

$$Z_{l_{11}}^{sem} = \left(\mathfrak{Z}_{sem_{out}} - \frac{\mathfrak{Z}_{sem_m}^{\ 2}}{\mathfrak{Z}_{core_{out}} + \mathfrak{Z}_{sem_{in}}}\right) + \mathfrak{Z}_{sh_{in}} + \mathfrak{Z}_{ins1} \quad (11)$$

It is seen that the expression of $Z_{l_{11}}^{sem}$ contains component impedance terms of the semiconducting screen, which ensures that the effect of the semiconducting screen is included in the expressions of cable impedance.

From (8) the self impedance of loop 2 ($Z_{l_{22}}^{sem}$) between sheath and external return (here Earth) is given by,

$$Z_{l_{22}}^{sem} = \mathfrak{Z}_{sh_{out}} + \mathfrak{Z}_{ins2} + Z_e \quad (12)$$

The mutual impedance ($Z_{l_{12}}^{sem}$) between loop 1 & 2 from (8) & (10) is given by,

$$Z_{l_{12}}^{sem} = Z_{l_{21}}^{sem} = -\mathfrak{Z}_{sh_m} \quad (13)$$

The equations (11) to (13) give complete impedance of cable with semiconducting screen in mesh domain which matches considerably with the impedance expressions obtained using the electromagnetic theory of double layered conductor in existing literature [13, 14]. It shows the accuracy and robustness of the adopted method based on loop analysis. The complete impedance matrix of the cable with semiconducting screen in mesh domain is given by,

$$[Z_{mesh}^{sem}] = \begin{bmatrix} Z_{l_{11}}^{sem} & Z_{l_{12}}^{sem} \\ Z_{l_{21}}^{sem} & Z_{l_{22}}^{sem} \end{bmatrix} \quad (14)$$

The current and voltage in different layers of cable measured w.r.t ground are known as phase current and voltage respectively, which are actually propagated through the practical cable. So to study wave properties of the cable in terms of phase quantities, voltage-current relationship in mesh domain needs to be converted to phase domain as follows,

The voltage-current relationship in the cable with semiconducting screen in mesh domain, as derived in (8) & (10), are given by,

$$[V]_{mesh} = [I]_{mesh}[Z_{mesh}^{sem}] \quad (15)$$

where,

$$[V]_{mesh} = [\Delta V_2 \quad \Delta V_3]^T \quad (16)$$

$$[I]_{mesh} = [I_2 \quad I_3]^T \quad (17)$$

and, $[Z_{mesh}^{sem}]$ is given by (14).

In Fig. 2 I_{core}^{sem} & I_{sh} are the phase current, entering core-semiconductor assembly and sheath respectively whereas V_{core}^{sem} & V_{sh} are respectively the phase voltage measured from ground to core-semiconductor assembly and sheath. The relationships between mesh and phase domain voltage and current can be obtained from Fig.2 as follows,

$$I_2 = I_{core}^{sem} \quad \& \quad I_3 = I_{core}^{sem} + I_{sh} \quad (18)$$

$$\Delta V_2 = V_{core}^{sem} - V_{sh} \quad \& \quad \Delta V_3 = V_{sh} \quad (19)$$

Putting (17) & (18) in (14) gives,

$$\begin{bmatrix} V_{core}^{sem} - V_{sh} \\ V_{sh} \end{bmatrix} = [Z_{mesh}^{sem}] \begin{bmatrix} I_{core}^{sem} \\ I_{core}^{sem} + I_{sh} \end{bmatrix} \quad (20)$$

Putting (9) on (15) and performing the row operations $R_1 \rightarrow R_1 + R_2$ on both sides of (17) and then multiplying and decomposing the quantities on LHS of (20) gives-

Table- I: Parameters for 500 kV cable [13]

Cable Layer	Relative Permittivity	Resistivity	Relative Permeability
Core Conductor	1	1.82×10^{-8}	1
Sheath Conductor	1	2.83×10^{-8}	1
Inner insulation	3.1	∞	0
Outer Insulation	4	∞	0
Semiconducting screen	variable	variable	1
r_{co}=30.45, r_{si}=71.15, r_{so}=74.8, r_{io}= 81.61, d =variable (*all dimensions are in mm*)			

$$\begin{bmatrix} V_{core}^{sem} \\ V_{sh} \end{bmatrix} = \begin{bmatrix} Z_{Ph_{11}}^{sem} & Z_{Ph_{12}}^{sem} \\ Z_{Ph_{21}}^{sem} & Z_{Ph_{22}}^{sem} \end{bmatrix} \begin{bmatrix} I_{core}^{sem} \\ I_{sh} \end{bmatrix} \quad (21)$$

where,

$Z_{Ph_{11}}^{sem}$ =Self impedance of core-semiconductor assembly *w.r.t* ground

$$= Z_{l_{11}}^{sem} + Z_{l_{22}}^{sem} + 2Z_{l_{12}}^{sem}$$

$$= \mathfrak{Z}_{sem_{out}} - \frac{\mathfrak{Z}_{sem_m}^2}{\mathfrak{Z}_{core_{out}} + \mathfrak{Z}_{sem_{in}}} + \mathfrak{Z}_{ins1} + \mathfrak{Z}_{sh_{in}} - \mathfrak{Z}_{sh_{out}} - \mathfrak{Z}_{ins2} - 2\mathfrak{Z}_{sh_m} \quad (22)$$

$Z_{Ph_{22}}^{sem}$ =Self impedance of sheath *w.r.t* ground

$$= Z_{l_{22}}^{sem} = \mathfrak{Z}_{sh_{out}} + \mathfrak{Z}_{ins2} \quad (23)$$

$Z_{Ph_{12}}^{sem} = Z_{Ph_{21}}^{sem}$ = Mutual impedance between core and sheath *w.r.t* ground

$$= Z_{l_{22}}^{sem} + Z_{l_{12}}^{sem} = \mathfrak{Z}_{sh_{out}} + \mathfrak{Z}_{ins2} - \mathfrak{Z}_{sh_m} \quad (24)$$

Therefore (22) to (24) give complete impedance of cable with semiconducting screen in phase domain which characterizes the wave propagation through the cable.

C. Admittance of cable with semiconducting screen

As the propagation through the central conductor is considered for analysis here, the effective admittance between core and sheath (Y_e) of the cable in Fig.1 can be determined from [13] as follows,

$$Y_e = \frac{1}{\frac{1}{y_{ins1}} + \frac{1}{y_{sem}}} = G_e + j\omega C_e \quad (25)$$

where G_e & C_e are the overall conductance & capacitance of cable with semiconducting screen respectively.

Published By:
Blue Eyes Intelligence Engineering
and Sciences Publication (BEIESP)

y_{sem} =Admittance of the semiconducting screen on the core outer surface

$$= \frac{j\omega\varepsilon_0\varepsilon_{sem}}{\ln\frac{r_{out}}{r_{in}}} \;\&\; \varepsilon_{sem} = \varepsilon_{rsem} + \frac{1}{j\omega\rho_{sem}} \quad (26)$$

where,

ε_{rsem} =relative permittivity of semiconducting material

ρ_{sem} = resistivity of semiconducting material

y_{ins1} = admittance of the insulating layer between semiconducting screen and sheath

$$= \frac{j\omega\varepsilon_0\varepsilon_{rins1}}{ln\frac{r_{out}}{r_{in}}} \text{ where } \varepsilon_{rins1} = \varepsilon_r^{'} - j\varepsilon_r^{"} \quad (27)$$

$\omega = 2\pi f; f$ = frequency of the propagated signal.

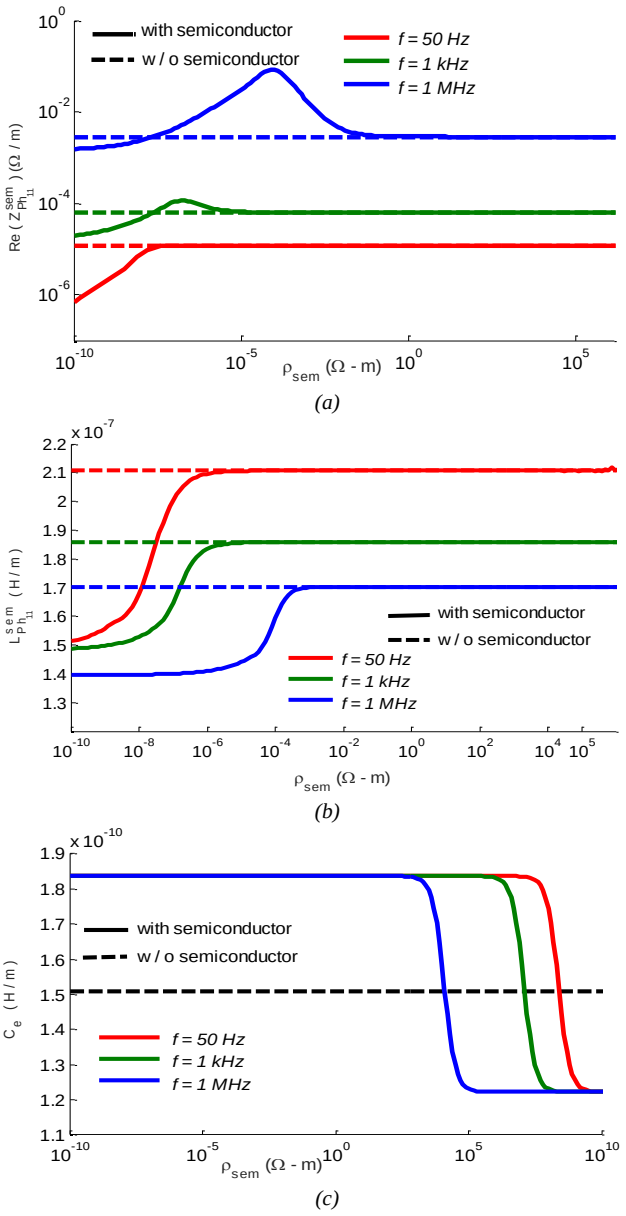

Fig. 3. Variation with semiconductor resistivity for different frequency: (a) Resistive part (Re ($Z_{Ph_{11}}^{sem}$)), (b) Inductive part ($L_{Ph_{11}}^{sem}$), (c) Capacitive part (C_e)

III. Result & Discussion

All geometric, electrical and magnetic properties of a single core (SC) 500 kV cable containing semiconducting screen on core outer surface as shown in Fig.1 are furnished in Table. 1. The effects of the variation of different parameters of the semiconducting screen and signal frequency on line parameters and wave properties of the cable are shown and analyzed below.

A. Cable line parameters

Only coaxial mode of wave propagation through the central conductor of the cable is considered for analysis which is governed by the self impedance ($Z_{Ph_{11}}^{sem}$) of core-semiconductor assembly and the effective admittance (Y_e) between core and sheath obtained from (22) and (25), respectively. Therefore all three line parameters of the cable namely resistive (*Re* ($Z_{Ph_{11}}^{sem}$)) & inductive ($L_{Ph_{11}}^{sem}$) part obtained from $Z_{Ph_{11}}^{sem}$ and effective capacitance (C_e) obtained from Y_e are considered here for analysis.

Variation with semiconductor resistivity (ρ_{sem}) for different frequency:

Fig. 3(*a*), (*b*) & (*c*) respectively show the variation of resistive (*Re* ($Z_{Ph_{11}}^{sem}$)), inductive ($L_{Ph_{11}}^{sem}$) and capacitive (C_e) part of the cable containing semiconducting screen as a function of semiconductor resistivity for different frequencies and compare it with that of the cable without semiconducting screen. The thickness of the semiconducting screen (*d*) is fixed at 5 mm.

At low frequency current mainly flows along the core conductor even when ρ_{sem} is in the range of core resistivity. As a result, *Re* ($Z_{Ph_{11}}^{sem}$) of the cable with semiconducting screen has a lower magnitude compared to that of the cable without semiconductor as shown in Fig. 3(*a*). But with the increase in frequency current redistributes towards the core surface due to skin effect and enters the semiconducting region. As a result, *Re* ($Z_{Ph_{11}}^{sem}$) of cable with semiconducting screen is increasing with the increase of ρ_{sem} and reaches the maxima at a particular value of ρ_{sem} as shown in Fig. 3(*a*). It is obtained from Fig. 3(*a*) that maxima of *Re* ($Z_{Ph_{11}}^{sem}$) for frequency 1 kHz and 1 MHz occurs at the resistivity 1.973×10^{-7} Ω - *m* and 1.973×10^{-4} Ω - *m* respectively. When these resistivity values are put in the expression of skin depth (δ), given by [13],

$$\delta = \sqrt{\frac{\rho}{\omega\mu}} \quad (27)$$

skin depth comes out almost equal to 5 mm, which is the thickness of the semiconducting screen considered here. Thus it indicates that for a particular frequency *Re* ($Z_{Ph_{11}}^{sem}$) reaches maxima at the value of ρ_{sem} for which skin depth would be almost equal to the semiconducting screen thickness. Therefore it can be said that with the increase in frequency, more current flows in the semiconducting region and higher resistivity is required to make skin depth equal to *d*. As a result, higher the frequency, higher is the value of ρ_{sem} at which maxima of *Re* ($Z_{Ph_{11}}^{sem}$) takes place, as shown in Fig. 3(*a*). When ρ_{sem} becomes much higher than the core resistivity, current mainly flows through the core even at high frequency and *Re* ($Z_{Ph_{11}}^{sem}$) settles to the value of the resistance provided by core alone, as seen in Fig. 3(*a*).

At a particular frequency inductance of the cable without semiconducting screen is the maximum inductance at that frequency and its magnitude decreases with the increase in frequency as shown in Fig. 3(*b*).

Retrieval Number: D7452118419/2019©BEIESP
DOI:10.35940/ijrte.D7452.118419
Journal Website: www.ijrte.org

Published By:
Blue Eyes Intelligence Engineering and Sciences Publication (BEIESP)

But in a cable with semiconducting screen, when ρ_{sem} is much smaller than the core resistivity, most of the current flow through the semiconductor region even at the low frequency. Thus the flux linkage takes place between the outer surface of semiconducting screen and the inner surface of sheath. It makes the area of flux linkage and thus $L_{Ph_{11}}^{sem}$ of the cable much lower than that of the cable without semiconducting screen at that frequency as shown in Fig. 3(*b*). With the increase of ρ_{sem}, current starts migrating away from the outer surface of the semiconducting screen.

Therefore the area of flux linkage is increasing which in turn increases the value of $L_{Ph_{11}}^{sem}$ with ρ_{sem} as seen in Fig. 3(*b*). When ρ_{sem} increases to the value at which $\delta \approx d$ as per (27), axial current starts flowing along the core outer surface. Thus $L_{Ph_{11}}^{sem}$ of the cable is

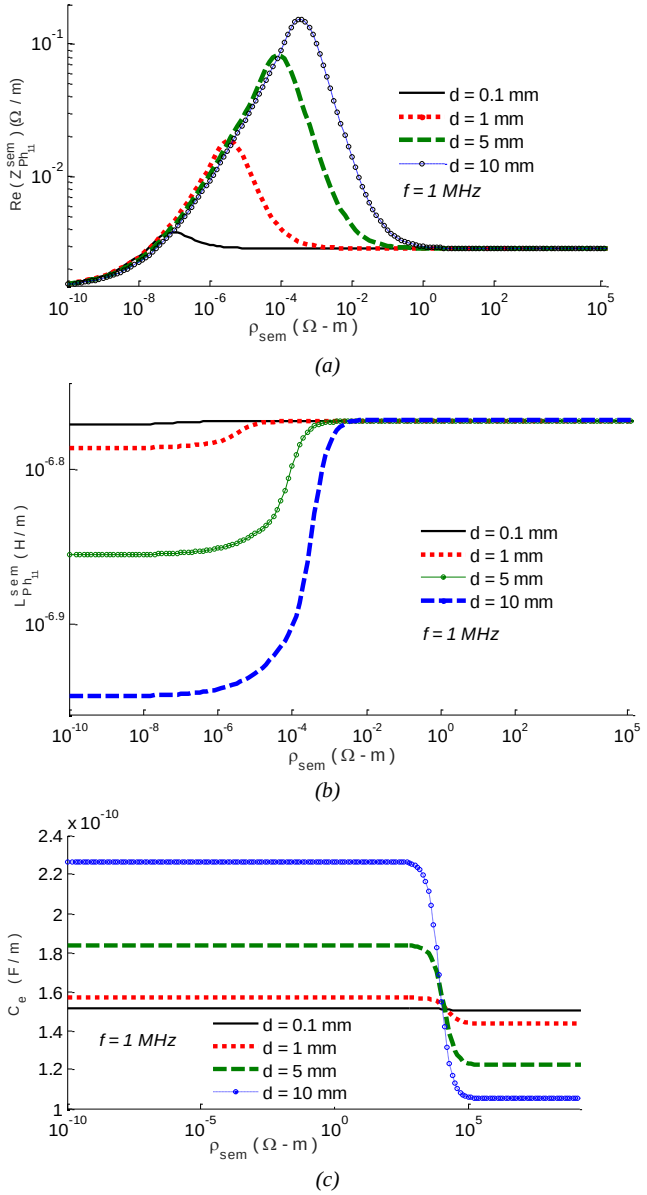

Fig. 4.Variation with semiconductor resistivity for different thickness: (a) Resistive part (Re ($Z_{Ph_{11}}^{sem}$)), (b) Inductive part ($L_{Ph_{11}}^{sem}$), (c) Capacitive part (C_e)

now determined by the flux linkage between the core outer and sheath inner surface which is the inductance of the cable without semiconductor at that frequency and remains fixed there with the further increase of ρ_{sem} as seen in Fig. 3*(b)*.

Also, higher the frequency, higher amount of current resides in the semiconducting region. Thus higher value of ρ_{sem} is needed to make current returning to the core outer surface. As a result, ρ_{sem} at which $L_{Ph_{11}}^{sem}$ reached the maximum value increases with the increase in frequency, as shown in Fig. 3(*b*).

At a particular frequency, charges are mainly accumulated on the outer surface of core-semiconductor assembly and the inner surface of the sheath in the cable with semiconducting screen when ρ_{sem} is lower than the core resistivity. Thus C_e is determined by the main insulator alone of the cable and remains constant for this range of ρ_{sem} as shown in Fig. 3(*c*). But when ρ_{sem} becomes more than the core resistivity, charge use to migrate towards the core outer surface. Therefore the effective value of C_e is determined by the series combination of capacitance provided by semiconducting screen and main insulator together which is lesser than the value of C_e provided by the main insulator alone. As a result, C_e is seen to be decreasing with ρ_{sem} in Fig. 3*(c)*. When the value of ρ_{sem} becomes so high that charges mainly accumulate on core outer and sheath inner surface, the effective value of C_e becomes fixed to the lowest value equal to the effective capacitance between core outer and sheath inner surface of the cable as shown in Fig. 3(*c*). Also, higher the frequency, higher amount of charge resides in the semiconductor region and higher ρ_{sem} is required to send the charge from semiconductor to conducting region. As a result, higher the frequency, higher is the value of ρ_{sem} at which decrease in C_e initiates as shown in Fig. 3(*c*).

The above discussions show that there is no significant difference between the resistive component of the cable with and without semiconducting screen both for very small and high range of semiconductor resistivity even at very high frequency. It indicates that for this range of resistivity semiconducting screen will have minimal effect on attenuation characteristics of the cable even at very high frequency. Also, the inductive component of the cable with semiconducting screen is varying at a lower range of ρ_{sem} but becomes almost independent of ρ_{sem} for higher range, especially at high frequency. But the capacitive part of the cable with semiconducting screen shows the inverse variation with ρ_{sem} compared to the inductive part. Therefore it can be said that the wave propagation velocity of the cable with semiconducting screen may depend on the inductive part of the cable at a lower range of ρ_{sem} whereas the velocity may be governed by the capacitive part for high values of ρ_{sem}, especially at high frequency.

Variation with semiconductor resistivity (ρ_{sem}) for different thickness (d) of semiconducting screen: The variation of *Re* ($Z_{Ph_{11}}^{sem}$)), $L_{Ph_{11}}^{sem}$ and C_e of the cable as a function of semiconducting screen thicknesses (*d*) over a wide range of ρ_{sem} is shown in Fig. 4*(a), (b) & (c)* respectively with frequency kept fixed at 1 MHz. It is clear from (27) that at a particular frequency, skin depth (δ) increases with ρ_{sem} and maxima of *Re* ($Z_{Ph_{11}}^{sem}$) takes place when $\delta \approx d$. Therefore higher the value of *d*, maxima of *Re* ($Z_{Ph_{11}}^{sem}$)

takes place at higher value $s\ of\ \rho_{sem}$ which in turn increases the overall magnitude of $Re\ (Z_{Ph_{11}}^{sem})$ with the increase in d as shown in Fig. 4(a). But the thickness of the semiconducting screen cannot be increased indefinitely due to mechanical constraints.

Inductive part of the cable with semiconducting screen is determined by the flux linkage between the outer and the inner surface of semiconducting screen and sheath respectively for the lower range of ρ_{sem} especially at high frequency as discussed previously.

Now with the increase of the thickness of semiconducting screen, area of the flux linkage deceases. As a result, $L_{Ph_{11}}^{sem}$ also decreases with the increase of d for a lower range of ρ_{sem}, as shown in Fig. 4*(b)*. But with the increase of ρ_{sem}, $L_{Ph_{11}}^{sem}$ approaches the value of the inductance of cable without semiconducting screen at that frequency as discussed previously and becomes independent of the thickness as seen in Fig. 4*(b)*.

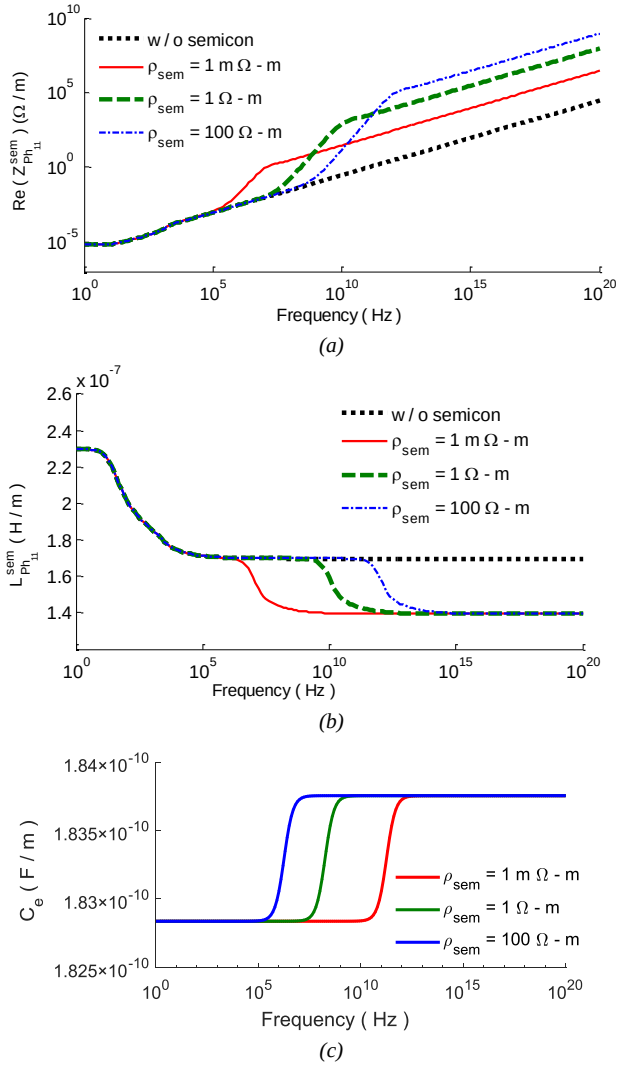

Fig. 5.Variation with frequency for different semiconductor resistivity: (a) Resistive part (Re ($Z_{Ph_{11}}^{sem}$)), (b) Inductive part ($L_{Ph_{11}}^{sem}$), (c) Capacitive part

It has been shown previously that C_e of the cable with semiconducting screen is decided by the main insulation alone for a certain range of ρ_{sem}, especially at high frequency. For this range of ρ_{sem}, thickness of the main insulation is relatively decreasing with the increase of d, which in turn increases C_e as shown in Fig. 4*(c)*. But with the increase of ρ_{sem} beyond this range, C_e is determined as a series combination of the capacitance of semiconducting screen and main insulation as discussed previously. Now higher the value of d, lower will be the capacitance provided by the semiconducting screen, which in turn reduces C_e. Therefore in this range of ρ_{sem}, higher the thickness of the semiconducting screen, higher is the rate of decrease in C_e, especially at high frequency, as shown in Fig. 4*(c)*.

The above discussion indicates that the effect of semiconducting screen on all three cable line parameter is minimal when it has a minimal thickness. For the lower range of semiconductor resistivity, inductive and capacitive part of the cable show inverse variation to each other with the increase in semiconducting screen thickness especially at high frequency. It indicates that the wave propagation velocity may become almost independent of the thickness of semiconducting screen for lower range of semiconductor resistivity.

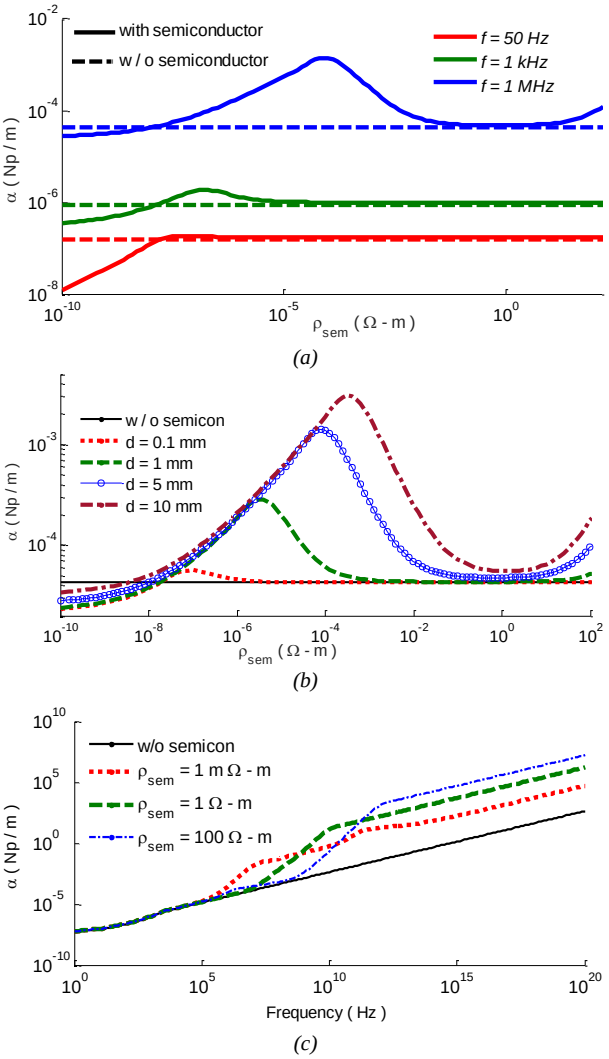

Fig. 6. Variation of α – (a) with ρ_{sem} for different frequency, (b) with ρ_{sem} for different thickness, (c) with frequency for different ρ_{sem}

Retrieval Number: D7452118419/2019©BEIESP
DOI:10.35940/ijrte.D7452.118419
Journal Website: www.ijrte.org

Published By:
Blue Eyes Intelligence Engineering and Sciences Publication (BEIESP)

Variation with frequency (f) for different semiconductor resistivity (ρ_{sem}): Fig. 5(*a*), (*b*) & (*c*) show the frequency variation of *Re* ($Z_{Ph_{11}}^{sem}$), $L_{Ph_{11}}^{sem}$ & C_e respectively of the cable for different ρ_{sem} keeping *d* fixed at 5mm and compare the same with that of cable without semiconducting screen. With the increase in frequency up to certain range (say 100 kHz), current migrates towards the outer surface of core conductor. As a result, there is no significant difference in the frequency variation of *Re* ($Z_{Ph_{11}}^{sem}$), $L_{Ph_{11}}^{sem}$ & C_e of the cable with and without semiconducting screen as shown in Fig. 5(*a*), (*b*) & (*c*) respectively.

But with the increase of *f* beyond this range current enter semiconducting region and there is respectively a sudden rise and fall in the value of *Re* ($Z_{Ph_{11}}^{sem}$) and $L_{Ph_{11}}^{sem}$ as shown in Fig. 5*(a)* & *(b)* respectively. It is also shown that the frequency at which this sudden change took place is increasing with the increase of ρ_{sem}, which is in accordance with the resistivity variation of these line parameters as discussed in the previous section.

B. Wave propagation characteristics

Wave propagation characteristics of the cable are determined by the propagation constant *(γ)* which is the function of impedance *(Z)* and admittance

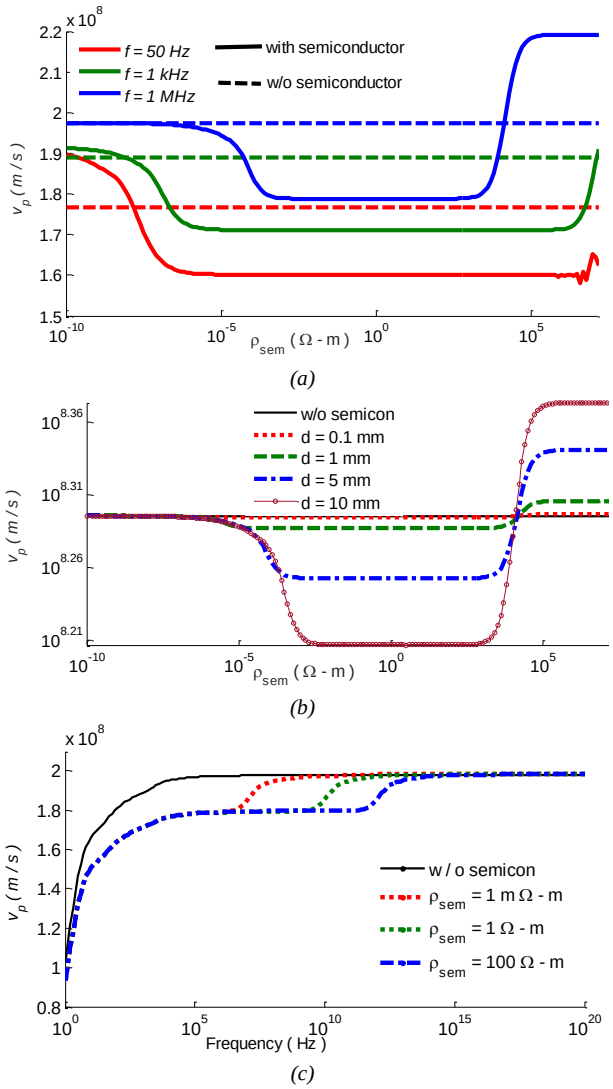

Fig. 8. Variation of v_p – (a) with ρ_{sem} for different frequency, (b) with ρ_{sem} for different thickness, (c) with frequency for different ρ_{sem}

(Y) of the cable given by,

$$\gamma = \sqrt{ZY} = \alpha + j\beta \quad (28)$$

where α and β represent the attenuation constant and phase constant of the cable, respectively. The variations of attenuation constant (α) and phase velocity (v_p) obtained from the phase constant of the cable with different electrical and physical properties of the semiconducting screen and frequency of the transmitted signal are discussed below.

Attenuation constant (α): The real part of γ in (28), known as the attenuation constant (α), is determined by the loss component of the cable. Thus α depends upon the resistive component of the cable and therefore influenced by the presence of semiconducting screen in cable structure.

Fig. 6(*a*) & (*b*) show the variation of α of the cable containing semiconducting screen with ρ_{sem} for different frequency (*f*) and semiconducting screen thickness (*d*) respectively and compare it with that of the cable without semiconducting screen. Both these variation of α resemble the variation of *Re* ($Z_{Ph_{11}}^{sem}$) of the cable depicted respectively in Fig. 4(*a*) & 5(*a*) as α is governed by the resistive component of the cable.

Just like *Re* ($Z_{Ph_{11}}^{sem}$), α of both the cable with and without semiconducting screen have almost same variation for very small and high range of ρ_{sem} at a particular frequency and semiconductor thickness as shown in Fig. 6(*a*) & (*b*). Also, with the increase of ρ_{sem} from very low value, α of the cable with semiconducting screen increases to reach the peak value and then decreases with further increase in ρ_{sem}. Like *Re* ($Z_{Ph_{11}}^{sem}$), the magnitude of α increases with the increase in *f* as well as *d* and higher the value of *f* and *d*, higher is the ρ_{sem} at which peak of α takes place as seen in Fig. 6(*a*) & (*b*) respectively for the same reason discussed previously for *Re* ($Z_{Ph_{11}}^{sem}$).

Frequency variation of α of the cable with semiconducting screen for different ρ_{sem} shown in Fig. 6(*c*) resembles the frequency variation of *Re* ($Z_{Ph_{11}}^{sem}$) as depicted in Fig. 5(*a*). Like *Re* ($Z_{Ph_{11}}^{sem}$), α in a cable with semiconducting screen becomes more than that in a cable without semiconducting screen for frequency higher than almost 100 kHz. Also higher the ρ_{sem}, higher is the rate and magnitude of increase in α, especially at high frequency range as shown in Fig. 6(*c*) for the same reason discussed for *Re* ($Z_{Ph_{11}}^{sem}$) in the previous section.

Above discussion shows that the semiconducting screen has minimal influence on attenuation characteristics both at a very low and high range of semiconductor resistivity as well as for minimal thickness of semiconducting screen even at a high frequency. But maximum attenuation at a particular frequency can be achieved for semiconductor resistivity at which skin depth becomes equal to thickness of semiconducting screen. This maximum magnitude can be increased by increasing the thickness as predicted from the pattern of resistive part of the cable with semiconducting screen discussed previously.

Retrieval Number: D7452118419/2019©BEIESP
DOI:10.35940/ijrte.D7452.118419
Journal Website: www.ijrte.org

Published By:
Blue Eyes Intelligence Engineering and Sciences Publication (BEIESP)

Phase velocity (v_p) The phase velocity (v_p) of the propagation can be determined from β in (28) as follows,

$v_p = \frac{\omega}{\beta}$ where $\omega = 2\pi f$

As the imaginary part of propagation constant determines the phase of a signal, the phase velocity has an inverse relationship with inductive (L) and capacitive (C) part of the cable given by,

$$v_p = \frac{1}{\sqrt{LC}} \quad (29)$$

Therefore the presence of semiconducting screen in cable structure has influence on v_p, which is studied below.

Fig. 7(a) shows the variation of v_p of the cable with semiconducting screen as a function of ρ_{sem} for different frequency (f) and compares it with that of the cable without semiconducting screen. As discussed previously that at a very low value of resistivity, the variation of $L_{Ph_{11}}^{sem}$ and C_e with ρ_{sem} has inverse nature of each other as given in Fig. 3(b) & (c) respectively. It makes v_p almost independent of semiconductor resistivity for this range of ρ_{sem} as per (29) even at high frequency as shown in Fig. 7*(a)*. With the increase of ρ_{sem}, $L_{Ph_{11}}^{sem}$ starts increasing, but C_e remains constant at a high value which results in a gradual decrease in v_p. After this resistivity range, $L_{Ph_{11}}^{sem}$ becomes almost fixed to the maximum value, whereas C_e is already constant to the high value, which makes v_p to be fixed at a low value as per (29). However, at the very high range of ρ_{sem}, though $L_{Ph_{11}}^{sem}$ remains constant at the high value, C_e starts decreasing as seen in Fig. 3(c) which brings sudden increase in $v_p$beyond the value of v_p of the cable without semiconducting screen, as shown in Fig. 7(a). Also, it is seen in Fig. 3(b) & (c) respectively that with the increase in frequency $L_{Ph_{11}}^{sem}$ decreases, but C_e remains unfazed which makes v_p increases with the increase in frequency, as shown in Fig. 7*(a)*.

It is shown in Fig. 7(b) that v_p of the cable with semiconducting screen remains almost independent of the variation of semiconducting screen thickness (d) for the very low range of ρ_{sem}. This is because the variation of $L_{Ph_{11}}^{sem}$ and C_e of the cable with d has inverse characteristics of each other in this range of ρ_{sem} as seen from Fig. 4(b) & (c) respectively. For ρ_{sem} beyond this range, both $L_{Ph_{11}}^{sem}$ and C_e are increasing with the increase in d, which results in the decrease in v_p with increasing d as shown in Fig. 7(b). For a very high range of resistivity, $L_{Ph_{11}}^{sem}$ becomes almost independent of d but $C_e$decreases with the increase in d. As a result, v_p increases with the increase in d beyond the velocity of the cable without semiconducting screen for this range of resistivity, as shown in Fig. 7(b).

Fig. 7(c) shows and compares the frequency variation of v_p between the cable with and without semiconducting screen for different ρ_{sem}. It shows that there is no significant difference in v_p of the cable with and without semiconducting screen at a very low range of frequency as both inductive and capacitive part of the cable with semiconducting screen remains independent of $\rho_{sem}$for this range of frequency. With the increase in frequency beyond this range, v_p of the cable with semiconducting screen has lower rate and magnitude of increase than that in the cable without semiconductor because $L_{Ph_{11}}^{sem}$ of the cable tends to become constant while C_e starts increasing to the maximum value as shown in Fig. 5(b) & (c) respectively. With further increase in frequency, v_p of the cable with semiconducting screen starts increasing at a higher rate to reach the velocity of the cable without semiconductor as shown in Fig. 7(c). Also Fig. 7(c) shows that higher the value of ρ_{sem}, higher is the frequency at which this increase in v_p of the cable with semiconducting screen takes place. At very high frequency range, v_p of the cable with semiconducting screen is seen to cross the velocity of cable without semiconducting screen due to the very low value of $L_{Ph_{11}}^{sem}$.

Above discussions indicates that the semiconducting screen has minimal effect on the propagation velocity of the cable when semiconductor resistivity is in the range of conductor resistivity and thickness is negligible even at high frequency. Also at lower range of semiconductor resistivity, velocity becomes a function of mainly the inductive part of the cable whereas at higher resistivity the velocity is mainly governed by capacitive part.

IV. CONCLUSION

A In this paper, the effects of the variations of the semiconducting screen properties on line parameters and wave properties of the cable are analyzed and compared with that of the cable without semiconducting screen. A method based on loop current analysis is adopted to derive the impedance and admittance of the cable considering the effect of the semiconducting screen. Using the derived expressions of impedance and admittance, a comparative analysis on the effects of the variation of geometric and electromagnetic properties of semiconducting screen on line parameters and wave properties of the cable with and without semiconducting screen is performed to draw the following inferences,

1. It is evident from the expressions of impedance that the semiconducting screen has its influence on self and mutual impedance of that conducting layer only to which it is attached.

2. The semiconducting screen has minimal effect on resistive part and rate of attenuation of the cable for very high and low ranges of resistivity, even at very high frequency. For the intermediate range of semiconductor resistivity, resistance and rate of attenuation of the cable increase considerably compared to that of the cable without semiconducting screen which is a desirable criterion for mitigating high frequency disturbances in the cable. At a particular frequency, maximum resistance and attenuation can be achieved for the resistivity, at which skin depth penetrates upto the semiconductor screen thickness. The peak value of the resistance and attenuation increases with the increase in frequency and thickness.

2. For very low semiconductor resistivity, inductance and capacitance of the cable show inverse variation to each other. It makes wave propagation velocity independent of resistivity. Beyond this range of resistivity, velocity becomes a function of inductance only and decreases with the resistivity compared to the velocity of the cable without semiconductor.

Retrieval Number: D7452118419/2019©BEIESP
DOI:10.35940/ijrte.D7452.118419
Journal Website: www.ijrte.org

Published By:
Blue Eyes Intelligence Engineering and Sciences Publication (BEIESP)

The rate of decrease increases with the increase in frequency and semiconductor thickness. On the other hand at a very high range of semiconductor resistivity, velocity is mainly governed by the capacitive part of the cable especially at high frequency and increases to the value higher than the velocity of the cable without semiconductor. The magnitude of increase in the velocity increases with the thickness of semiconducting screen.

3. For very thin semiconducting screen, its effect on line parameters and wave properties of the cable becomes minimal for any resistivity even at high frequency.

Thus by altering geometric and electromagnetic properties of the semiconducting screen, the wave propagation characteristics of the cable can be varied to improve high frequency behavior of the cable.

REFERENCES

1. A. Ametani, "A general formulation of impedance and admittance of cables," *IEEE Trans. Power App. Syst.*, vol. PAS-99, no. 3, pp. 902–910, May 1980, doi: 10.1109/TPAS.1980.319718.
2. S. A. Schelkunoff, "The electromagnetic theory of coaxial transmission line and cylindrical shields," *Bell Syst. Tech. J.*, vol. 13, pp. 532–579, 1934.
3. N Nagaoka, A Ametani, "A development of a generalized frequency-domain transient program-FTP," *IEEE Trans. Power App. Syst.*, vol. 3, no. 4, pp. 1996-2004, Oct. 1988.
4. G. E. Bridges, "Transient plane wave coupling to bare and insulated cables buried in a lossy half-space," *IEEE Trans. Electromagn. Compat..*, vol. 37, no. 1, pp. 62-70, Feb. 1995.
5. J. C. L. V. Silva, A. C. S. Lima, A. P. C. Magalhães and M. T. Correia de Barros, "Modelling seabed buried cables for electromagnetic transient analysis," *IET GENER TRANSM DIS*, vol. 11, no. 6, pp. 1575-1582, 20 4 2017.
6. X. Liu, C. Ti and G. Liang, "Wide-band modelling and transient analysis of the multi-conductor transmission lines system considering the frequency-dependent parameters based on the fractional calculus theory," *IET GENER TRANSM DIS*, vol. 10, no. 13, pp. 3374-3384, 6 10 2016..
7. B. Gustavsen and J. Sletbak, "Transient sheath overvoltages in armoured power cables," *IEEE Trans. Power Del.*, vol. 11, no. 3, pp. 1594-1600, July 1996.
8. S. A. Boggs, A. Pathak, P. Walker, "Partial discharge XXII: high frequency attenuation in shielded solid dielectric power cable and implications thereof for PD location," *IEEE Electr. Insul. Mag.*, vol. 12, no. 1, pp. 9-16, Jan.-Feb. 1996.
9. B. Gustavsen, "Panel session on data for modeling system transients insulated cables," *Proc. IEEE Power Engineering Society Winter Meeting*, Columbus, OH, USA, 2001, pp. 718-723. 10.1109/PESW.2001.916943
10. G. Mugala, R. Eriksson, U. Gäfvert, P. Pettersson, "Measurement technique for high frequency characterization of semi-conducting materials in extruded cables," *IEEE Trans. Dielectr. Electr. Insul*, vol. 11, no. 3, pp. 471-480, July 2004.
11. Tanabe, Nobuhiro & Baba, Yoshihiro & Nagaoka, Naoto & Ametani, Akihiro. (2001). A Transient Analysis of a Cable with a Two-Layer Conductor by FDTD Method. IEEJ Transactions on Power and Energy.
12. T. Noda and S. Yokoyama, "Thin wire representation in finite difference time domain surge simulation," *IEEE Trans. Power Del.*, vol. 17, no. 3, pp. 840-847, July 2002.
13. N. Amekawa, A. Ametani, Y. Baba, N. Nagaoka, "Derivation of a semiconducting layer impedance and its effect on wave propagation characteristics on a cable," *IEEE Trans. Power Del.*, vol. 19, no. 4, pp.1523-1531, July 2003.
14. A. Ametani, Y. Miyamoto, N. Nagaoka, "Semiconducting layer impedance and its effect on cable wave-propagation and transient characteristic," *IEEE Trans. Power Del.*, vol. 19, no. 4, pp.1523-1531, Oct. 2004.
15. M. Hasheminezhad, M. Vakilian, T. R. Blackburn and B. t. Phung, "Direct Introduction of Semicon Layers in XLPE Cable Model," *2006 International Conference on Power System Technology*, Chongqing, 2006, pp. 1-7.
16. Y. Baba, N. Tanabe, N. Nagaoka and A. Ametani, "Transient analysis of a cable with low-conducting layers by a finite-difference time-domain method," *IEEE Trans. Electromagn. Compat..*, vol. 46, no. 3, pp. 488-493, Aug. 2004.
17. G M. Hashmi, R. Papazyan, M. Lehtonen, "Determining wave propagation characteristics of MV XLPE power cable using time domain reflectometry technique," *Turk. J. Elec. Eng. & Comp. Sci.*, vol. 19, no. 2, pp.159-163, 2011.
18. R. Paludo, G. C. da Silva, V. S. Filho, "The study of semiconductor layer effect on underground cables with Time Domain Reflectometry (TDR)," *IOSR-JEEE*, vol. 7, no. 6, pp.01-07, 2013.
19. G. Mugala, R. Eriksson, P. Pettersson, " Comparing two measurement techniques for high frequency characterization of power cable semiconducting and insulating materials," *IEEE Trans. Dielectr. Electr. Insul*, vol. 13, no. 4, pp. 712 – 716, Aug. 2006.
20. G. Mugala, R. Eriksson, U. Gäfvert, P. Pettersson, "Measurement technique for high frequency characterization of semi-conducting materials in extruded cables," *IEEE Trans. Dielectr. Electr. Insul*, vol. 11, no. 3, pp. 471-480, July 2004.

AUTHORS PROFILE

Swarnankur Ghosh, received his M.Tech degree in Electrical engineering in 2012 from Jalpaiguri Govt. Engineering College, Jalpaiguri, West Bengal, India. He is currently pursuing PhD in the area of high voltage engineering under Department of Electrical engineering, National Institute of Technology Meghalaya, Meghalaya, India. His research interests include transients modelling of UG Cable, wave propagation through cable, lightning transient, numerical computation of electrical field.

Supriyo Das, received the Master degree from the Indian Institute of Technology Madras and Ph.D. from Indian Institute of Technology Kanpur, India, both in electrical engineering in 2004 and 2014 respectively. He is currently working as an Assistant Professor in the Department of Electrical Engineering at National Institute of Technology Meghalaya, India His research interests include assessment and characterization of polymeric dielectrics, transient analysis, lightning phenomena in electrical system.